

Relationship Between Paravascular Abnormalities and Choroidal Thickness in Young Highly Myopic Adults

Menghan Li^{1,2,*}, Luyao Ye^{1,2,*}, Guangyi Hu^{1,2}, Qiuying Chen^{1,2}, Dandan Sun^{1,2}, Haidong Zou^{1,2}, Jiangnan He¹, Jianfeng Zhu^{1,†}, Ying Fan^{2,†}, and Xun Xu^{1,2}

¹ Department of Preventative Ophthalmology, Shanghai Eye Disease Prevention and Treatment Center, Shanghai Eye Hospital, Shanghai, China

² Department of Ophthalmology, Shanghai General Hospital, Shanghai Jiao Tong University School of Medicine, National Clinical Research Center for Eye Diseases, Shanghai Key Laboratory of Ocular Fundus Diseases, Shanghai Engineering Center for Visual Science and Photo Medicine, Shanghai Engineering Center for Precise Diagnosis and Treatment of Eye Diseases, Shanghai, China

Correspondence: Ying Fan, Department of Ophthalmology, Shanghai General Hospital, Shanghai Jiao Tong University School of Medicine, No. 100 Haining Road, Shanghai 200080, China. e-mail: mdfanying@sjtu.edu.cn
Jianfeng Zhu, Department of Preventative Ophthalmology, Shanghai Eye Disease Prevention and Treatment Center, No. 380 Kangding Road, Shanghai 200040, China. e-mail: jfzhu1974@hotmail.com

Received: March 14, 2022

Accepted: May 24, 2022

Published: June 21, 2022

Keywords: paravascular abnormalities; choroidal thickness; high myopia; retinoschisis; risk factors

Citation: Li M, Ye L, Hu G, Chen Q, Sun D, Zou H, He J, Zhu J, Fan Y, Xu X. Relationship between paravascular abnormalities and choroidal thickness in young highly myopic adults. *Transl Vis Sci Technol.* 2022;11(6):18, <https://doi.org/10.1167/tvst.11.6.18>

Purpose: The purpose of this study was to investigate the clinical characteristics of paravascular abnormalities (PVAs) and retinoschisis, and their associations with choroidal thickness (ChT) in young highly myopic (HM) adults.

Methods: A total number of 645 eyes were included. Paravascular microfolds (PMs), paravascular cystoid spaces (PCs), paravascular lamellar holes (PLHs), and retinoschisis were detected using swept-source optical coherence tomography. Their associations with macular ChT and risk factors were analyzed.

Results: PMs, PCs, and PLHs were detected in 203 (31.5%), 141 (21.9%), and 30 (4.7%) eyes, respectively. Retinoschisis was found in 50 (7.8%) eyes, 43 (86.0%) of which were located around the retinal vessels surrounding the optic disc. A decreasing trend of macular ChT ($P < 0.001$) was observed in the eyes with PMs only, with both PCs and PMs, and with PLHs, PCs, and PMs. After adjustments for age, sex, and axial length (AL), the presence of PCs, PLHs, or retinoschisis around the optic disc was negatively associated with macular ChT (all $P < 0.05$). Eyes with longer AL, incomplete posterior vitreous detachment (PVD), and myopic atrophic maculopathy (MAM) were more likely to have PCs (all $P < 0.01$) and retinoschisis around the optic disc (all $P < 0.05$).

Conclusions: PVAs were observed in approximately one third of the young HM adults in this study. The presence of PCs, PLHs, or retinoschisis around the optic disc was associated with thinner macular ChT. Eyes with longer AL, incomplete PVD, and MAM may be at risk of developing PVAs and retinoschisis around the optic disc.

Translational Relevance: PCs, PLHs, and retinoschisis around the optic disc could serve as early indicators for myopia progression.

Introduction

Paravascular abnormalities (PVAs) represent fundus lesions located around the retinal vessels, which occur most frequently in eyes with high myopia

or epiretinal membrane (ERM).^{1,2} Three types of PVAs have been defined and reported so far: vascular and paravascular microfolds (PMs; tenting projections of the retinal vessels toward the vitreous cavity), paravascular retinal cystoid spaces (PCs; hyporeflexive spaces around the retinal vessels within the inner

retina), and paravascular lamellar holes (PLHs; cracks extending from the internal limiting membrane to the partial thickness of the neural retina).^{3–5} Retinoschisis, a splitting of the retina in highly myopic (HM) eyes, has been reported in the macula and around the retinal vascular, which is defined as macular retinoschisis (MRS) and paravascular retinoschisis (PVRs), respectively.^{6,7} PVRs has also been included as a type of PVAs in some previous studies.^{7,8}

Several investigations have been focused on the distribution of PVAs and their relation to MRS in HM eyes, emphasizing the need for careful examinations and follow-up because of the possibility of transition into more severe lesions.^{6–10} Recent evidence showed that PVAs were already present at a young age and were caused by the tractional forces with bridging tissues between the vitreous cavity and retina.⁹ The choroidal thickness (ChT) decreases with the increase in the levels of myopia and is closely correlated with age, refractive diopter, and axial length (AL).^{11–15} ChT thinning plays an important role in the early stage of myopic maculopathy and might be a marker for the prediction of myopia progression.^{14,16,17} Therefore, it is important to explore the distribution and features of PVAs as early myopic lesions and their associations with ChT in young adults with HM.

In this study, we investigated the clinical characteristics and distribution of various types of PVAs and retinoschisis in young adults with HM. Their associations with macular ChT and risk factors were also analyzed.

Methods

Setting and Participants

The Shanghai High Myopia Study for Adults (SHMSA) is an ongoing HM cohort study which started in 2016 at the Shanghai Eye Diseases Prevention and Treatment Center in Shanghai, China. Details about this study are available in our previous publication.¹⁸ The protocol was approved by the Ethics Committee of Shanghai General People's Hospital, Shanghai Jiao Tong University School of Medicine, in compliance with the tenets of the Declaration of Helsinki. Written informed consent forms were signed by all participants.

All participants enrolled in the present study met the inclusion criteria: between 18 and 49 years old and with HM defined as spherical equivalent (SE) ≤ -6 D or AL ≥ 26 mm.¹⁹ The exclusion criteria were secondary myopia, intraocular pressure (IOP) > 21 mm

Hg, corneal opacity, severe cataract, glaucoma, fundus lesions unrelated to myopia (e.g. diabetic retinopathy, retinal vein occlusion, central serous chorioretinopathy, and optic neuropathy), systemic diseases with ocular involvement, history of eye surgery (except for cataract surgery), and poor-quality (a signal strength index ≤ 60) images.

Ophthalmic Examinations

All the participants underwent comprehensive clinical interviews and ophthalmic examinations, including slit-lamp biomicroscopy, assessment of SE using an autorefractor instrument (model KR-8900; Topcon, Tokyo, Japan), measurement of the IOP (Full Auto Tonometer TX-F; Topcon, Tokyo, Japan), AL measurement with an optical low-coherence reflectometer (Lenstar LS-900; Haag-Streit AG, Koenig, Switzerland), and swept-source optical coherence tomography (SS-OCT; model DRI OCT-1 Atlantis; Topcon, Tokyo, Japan). In the SS-OCT scanning protocols, we used a 12-line radial scan pattern centered on the fovea and the optic disc with a scan length of 9 mm and a 256-line 3-dimensional scan pattern with scan dimensions of $12 \times 9 \times 2.6$ mm³. An experienced optometrist performed the subjective refraction measurements in all participants. The SE was obtained as the spherical power plus a half of the cylindrical power.

Classifications and Definitions

Three types of PVAs, including PMs, PCs, and PLHs, were identified in the SS-OCT images obtained (Fig. 1). PVRs was defined as retinoschisis around the retinal vessels outside the macular region. The locations of PVRs around the optic disc were further observed (Supplementary Fig. S1). Incomplete posterior vitreous detachment (PVD) and ERM were identified as vitreoretinal abnormalities that cause inward traction.^{3,9,20–22}

Based on the new classification and grading system (ATN),¹⁹ myopic atrophy alterations were classified into 5 categories: A0, no maculopathy; A1, tessellated fundus; A2, diffuse chorioretinal atrophy; A3, patchy chorioretinal atrophy; and A4, macular atrophy. The eyes with a grade $\geq A2$ were defined as the presence of myopic atrophic maculopathy (MAM). The classifications were performed by two independent, well-trained graders. In each controversial case, adjudication was made by a retina specialist.

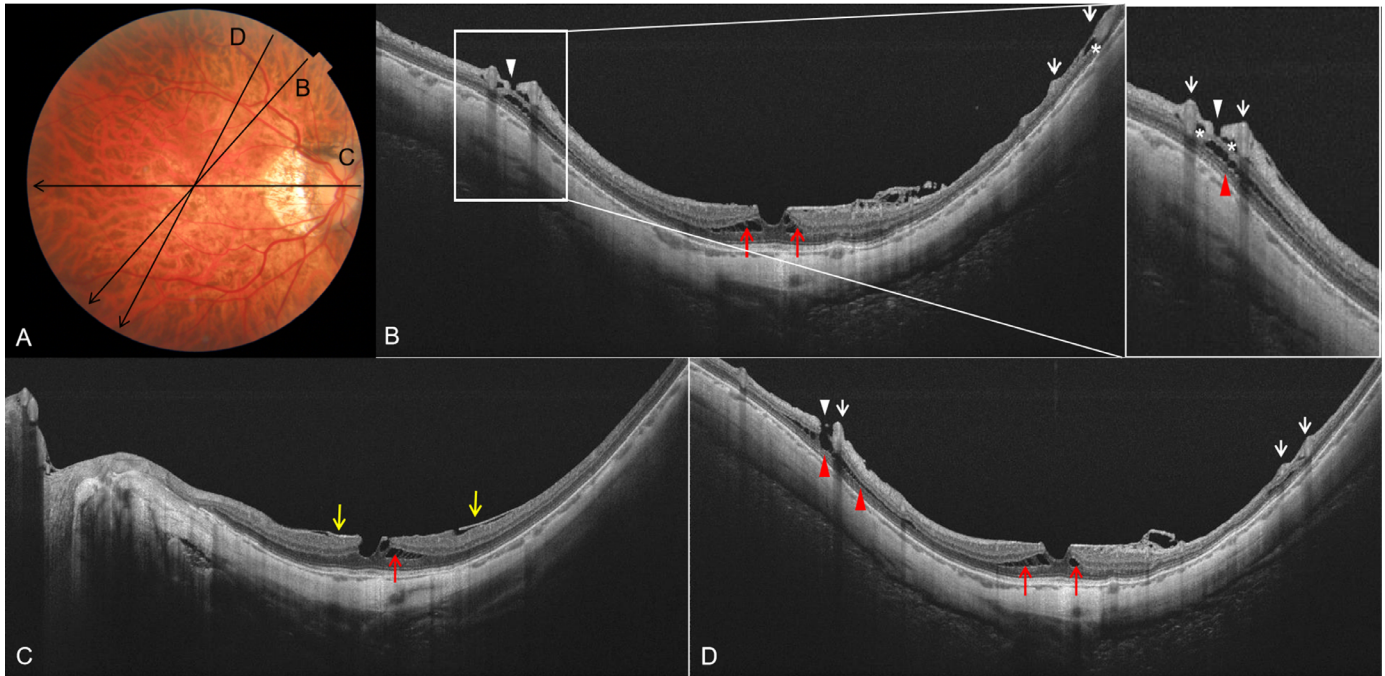


Figure 1. Fundus photograph and SS-OCT images of an eye with paravascular abnormalities and retinoschisis both around the vascular arcade (PVRs) and in the macula (MRS). **(A)** Right fundus photograph of a 49-year-old woman (axial length = 28.35 mm). **(B)** Oblique scan image showing paravascular microfolds (white arrows) and adjacent paravascular cystoid spaces (white asterisks). Fissure-like structure is observed around a retinal vessel, suggesting the presence of a paravascular lamellar hole (white arrowheads). An outer retinal splitting is also detected by SS-OCT, which suggests a PVRs (red arrowheads). **(C)** Horizontal scan image showing the epiretinal membrane (yellow arrows) and MRS (red arrows). **(D)** Oblique scan image showing an extending trend of PVRs (red arrowheads) toward the macula; MRS originated independently in the fovea (red arrows).

SS-OCT Imaging Measurements

The ChT, defined as the vertical distance between the Bruch's membrane and the choroid-sclera interface, was measured in SS-OCT as well. The tomography maps were overlaid with an Early Treatment Diabetic Retinopathy Study (ETDRS) grid that was focused on the fovea. The diameters of the foveal, parafoveal, and perifoveal circles of the ETDRS grid were 1, 3, and 6 mm, correspondingly, which were further subdivided into nasal, temporal, superior, and inferior quadrants. All nine sectors of the grid were applied in the macular region to obtain the average thickness.

Fundus Photography and Assessments

Fundus photographs centered on the fovea and the optic disc were obtained using the same SS-OCT with a digital, nonmydriatic retinal camera. The peripapillary atrophy (PPA) area was denoted as chorioretinal atrophy adjacent to the optic disc.^{23,24} The definition of the tilted optic disc was previously described as the tilt ratio of the minimum to the maximum disc diameter ≤ 0.80 .^{25,26} The tilt ratio and the PPA area were calculated from the fundus photographs using

ImageJ version 1.53 software (National Institutes of Health, Bethesda, MD, USA). The magnification of the fundus camera was $\times 1.4$, and the total magnification was calculated by integrating the magnification factor of ImageJ software. The area of the PPA was converted from pixels into millimeters squared. The lateral magnification was corrected using AL by the Littmann's formula.²⁷

Statistical Analysis

All statistical analyses were performed using SPSS software version 26 (IBM Corp., Armonk, NY, USA), and a 2-tailed value of $P < 0.05$ was considered to indicate statistically significant differences. Only the right eye of each participant was included for statistical analyses. The participants' characteristics were expressed as counts or proportions for the categorical data and as means \pm standard deviation (SD) for the continuous data. The distribution was assessed by the Kolmogorov-Smirnov test. The intergroup differences of the continuous data were tested using Student's t -test, Mann-Whitney U test, or Kruskal-Wallis test with Bonferroni's post hoc test. The frequency of the categorical variables was compared via the chi-square

test or Fisher’s exact test. The *P* value for the trend was calculated by univariate regression analysis. Multivariate linear regression analysis was also performed to determine the effects of PVAs and PVRs on macular ChT. Multivariate logistic regression was used to detect the risk factors.

Results

General Characteristics

Of the 658 right eyes that were initially screened in this study, 13 were excluded for the following reasons: 10 eyes had IOP >21 mm Hg; one had glaucoma; one had retinal pathology unrelated to high myopia; and one had a history of eye surgery other than cataract extraction. Finally, a total number of 645 right eyes of 645 participants (310 men and 335 women) were analyzed. The mean age was 29.13 ± 9.47 years, the mean SE was -7.38 ± 2.44 D, and the mean AL was 26.71 ± 1.00 mm.

Distribution and Features of PVAs and Their Associations With Macular ChT

On the SS-OCT images obtained, we detected PVAs in 203 (31.5%) of the 645 eyes. The participants with PVAs tended to be older ($P < 0.001$), with longer AL

($P < 0.001$), with lower SE ($P < 0.001$), with thinner macular ChT ($P < 0.001$), with larger PPA area ($P < 0.001$), and with higher rates of MAM ($P < 0.001$), incomplete PVD ($P < 0.001$), and ERM ($P = 0.005$; Table 1).

PMs, PCs, and PLHs were detected in 203 (31.5%), 141 (21.9%), and 30 (4.7%) eyes, respectively. We further divided the participants into 3 age groups and 3 AL groups: 26.0% of the eyes had PVAs in the 18 to 29 years age group; the proportion rose to 37.1% in the 30 to 39 years age group, and continued to increase to 41.6% in the 40 to 49 years age group. In the group with an AL value less than 26 mm, 24.6% had PVAs, and the proportion rose to 30.5% in the group with an AL between 26 and 28 mm; this increase continued to 50.8% in the group with an AL value of 28 mm or more. Upward trends in the percentages of the eyes with PMs, PCs, and PLHs were observed with aging (all $P < 0.01$) and AL elongation (all $P < 0.01$; Fig. 2).

All eyes with PCs co-existed with PMs, and all eyes with PLHs co-existed with PCs and PMs. The eyes with PMs only showed no difference in AL, SE, and macular ChT but had an older mean age ($P = 0.006$) than the eyes without PVAs. The eyes with both PCs and PMs, and the eyes with PLHs, PCs, and PMs had older mean age, longer AL, lower SE, and thinner macular ChT (all $P < 0.05$) than the eyes without PVAs (Table 2). A decreasing trend in macular ChT ($P < 0.001$) and SE ($P < 0.001$) but an increasing trend in AL ($P < 0.001$) and the presence of MAM ($P < 0.001$) were observed

Table 1. General Characteristics and Comparisons between the Eyes With and Without Paravascular Abnormalities

	All	Non-PVAs	PVAs	<i>P</i> Value
No. of the eyes	645	442	203	
Age, y	29.13 ± 9.47	28.08 ± 9.04	31.42 ± 9.98	<0.001
Sex (male/female)	310/335	220/222	90/113	0.20
AL, mm	26.71 ± 1.00	26.60 ± 0.92	26.90 ± 1.12	<0.001
SE, D	-7.38 ± 2.44	-7.06 ± 2.32	-8.06 ± 2.57	<0.001
IOP, mm Hg	14.60 ± 2.57	14.54 ± 2.57	14.72 ± 2.56	0.47
Macular ChT, μ m	181.51 ± 57.19	188.66 ± 55.72	165.94 ± 57.41	<0.001
Incomplete PVD, <i>n</i> (%)	325 (50.39)	195 (44.12)	136 (67.00)	<0.001
ERM, <i>n</i> (%)	7 (1.09)	1 (0.23)	6 (2.96)	0.005
MAM, <i>n</i> (%)	24 (3.72)	6 (1.36)	18 (8.87)	<0.001
Retinoschisis, <i>n</i> (%)	50 (7.75)	0 (0.00)	50 (24.63)	<0.001
PPA area, mm ²	0.53 ± 0.78	0.46 ± 0.71	0.69 ± 0.90	<0.001
Tilt ratio	0.81 ± 0.09	0.81 ± 0.09	0.81 ± 0.09	0.96

PVAs, paravascular abnormalities; AL, axial length; SE, spherical equivalent; D, diopter; IOP, intraocular pressure; ChT, choroidal thickness; PVD, posterior vitreous detachment; ERM, epiretinal membrane; MAM, myopic atrophic maculopathy; PPA, peripapillary atrophy.

The *P* values for the difference between PVAs and non-PVAs groups were by Mann-Whitney *U* test, chi-square test, or Fisher’s exact test, as appropriate.

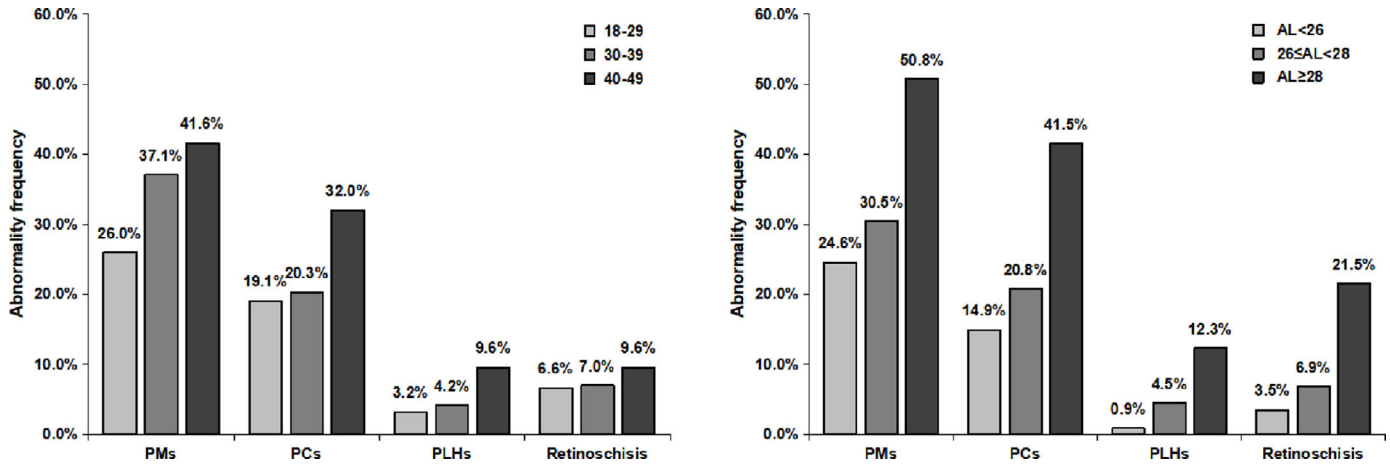


Figure 2. Percentages of the eyes with paravascular microfolds (PMs), paravascular cystoid spaces (PCs), paravascular lamellar holes (PLHs), and retinoschisis stratified by age (left) and axial length (right).

Table 2. Characteristics of the Eyes Without PVAs, With PMs only, With Both PCs and PMs, and With PLHs, PCs, and PMs

	Non-PVAs	PMs Only	PCs and PMs	PLHs, PCs, and PMs	P for Trend ^b	P Value ^c
No. of the eyes	442	62	111	30		
Age, y	28.08 ± 9.04	31.39 ± 9.17 ^a	30.69 ± 10.24 ^a	34.17 ± 10.48 ^a	0.001	0.44, 0.11, 0.35
Sex (male/female)	220/222	38/24	43/68 ^a	9/21 ^a	0.015	
AL, mm	26.60 ± 0.92	26.64 ± 1.02	26.99 ± 1.14 ^a	27.50 ± 1.05 ^a	<0.001	0.10, 0.009, <0.001
SE, D	-7.06 ± 2.32	-7.13 ± 2.28	-8.40 ± 2.40 ^a	-8.72 ± 3.24 ^a	<0.001	<0.001, 0.75, 0.004
Macular ChT, μm	188.66 ± 55.72	196.89 ± 60.23	158.57 ± 50.59 ^a	129.25 ± 44.39 ^a	<0.001	<0.001, 0.011, <0.001
MAM, n (%)	6 (1.36)	2 (3.23)	10 (9.01) ^a	6 (20.00) ^a	<0.001	
Retinoschisis	0 (0.00)	0 (0.00)	28 (25.23) ^a	22 (73.33) ^a	<0.001	

PVAs, paravascular abnormalities; PMs, paravascular microfolds; PCs, paravascular cystoid spaces; PLHs, paravascular lamellar holes; AL, axial length; SE, spherical equivalent; D, diopter; ChT, choroidal thickness; MAM, myopic atrophic maculopathy.

^aThe *P* < 0.05 for comparisons between non-PVAs groups and other three groups using the Mann-Whitney *U* test or chi-square test.

^bThe *P* values for trend using univariate regression analysis.

^cThe *P* values for the difference between eyes with PMs only and eyes with both PCs and PMs, eyes with both PCs and PMs and eyes with PLHs, PCs, and PMs, and eyes with PMs only and eyes with PLHs, PCs, and PMs using the Kruskal-Wallis test with the post hoc test.

in the eyes with PMs only, with both PCs and PMs and with PLHs, PCs, and PMs.

Next, multivariate linear regression analysis was performed to identify the independent factors associated with macular ChT. The model showed that the presence of both PCs and PMs, and the simultaneous presence of PLHs, PCs, and PMs were both independently associated with macular ChT after adjustments for age, sex, AL, and PPA area (both *P* = 0.001). However, the presence of PMs only was not associated with macular ChT. The combination of these factors yielded an adjusted *R*² of 0.208 (Table 3).

Using multivariate regression analysis, we further explored the risk factors for the presence of both PCs and PMs and concurrent presence of PLHs, PCs, and PMs. Significant factors associated with the presence of both PCs and PMs were female sex (odds ratio [OR] = 1.71, *P* = 0.024), longer AL (OR = 1.48, *P* = 0.001), the presence of incomplete PVD (OR = 1.91, *P* = 0.008), and the presence of MAM (OR = 4.54, *P* = 0.007). Statistically significant factors associated with the simultaneous presence of PLHs, PCs, and PMs were female sex (OR = 3.25, *P* = 0.016), longer AL (OR = 2.46, *P* < 0.001), and the presence of MAM (OR = 4.78, *P* = 0.039; Table 4). However, the presence of

Table 3. Multivariate Regression Analysis of Associated Factors with Macular Choroidal Thickness in All Subjects

Variables	β	Standard Error	P Value	VIF
Age, y	-0.05	0.24	0.83	1.23
Sex (female)	-23.56	4.20	<0.001	1.09
PVAs				
Non-PVAs	1.00 (Reference)			
PMs only	6.65	6.97	0.34	1.05
PCs and PMs	-18.30	5.54	0.001	1.09
PLHs, PCs, and PLHs	-34.12	9.96	0.001	1.10
AL, mm	-17.20	2.25	<0.001	1.26
PPA area, mm ²	-8.89	2.97	0.003	1.34

PVAs, paravascular abnormalities; PMs, paravascular microfolds; PCs, paravascular cystoid spaces; PLHs, paravascular lamellar holes; AL, axial length; PPA, peripapillary atrophy.

Table 4. Multivariate Regression Analysis of the Risk Factors Associated With Paravascular Abnormalities in the Different Groups

	Odds Ratio (95% Confidence Intervals)	P Value
PCs and PMs versus non-PVAs		
Age, y	1.01 (0.99–1.04)	0.27
Sex (female)	1.71 (1.07–2.71)	0.024
AL (per 1-mm increase)	1.48 (1.18–1.87)	0.001
Incomplete PVD	1.91 (1.19–3.07)	0.008
ERM	5.47 (0.48–62.28)	0.17
MAM	4.54 (1.51–13.66)	0.007
PLHs, PCs, and PMs versus non-PVAs		
Age, y	1.05 (1.0–1.10)	0.05
Sex (female)	3.25 (1.25–8.45)	0.016
AL (per 1-mm increase)	2.46 (1.57–3.84)	<0.001
Incomplete PVD	1.94 (0.80–4.75)	0.15
ERM	2.88 (0.17–48.02)	0.46
MAM	4.78 (1.08–21.12)	0.039

PVAs, paravascular abnormalities; PMs, paravascular microfolds; PCs, paravascular cystoid spaces; PLHs, paravascular lamellar holes; AL, axial length; PVD, posterior vitreous detachment; ERM, epiretinal membrane; MAM, myopic atrophic maculopathy.

incomplete PVD was not a risk factor for the concurrent presence of PLHs, PCs, and PMs.

Distribution and Features of Retinoschisis and its Association With Macular ChT

Retinoschisis was detected in 50 (7.8%) of 645 eyes. Forty-three (86.0%) of 50 eyes with retinoschisis were identified to be with PVRS around the optic disc, 4 (8.0%) eyes with PVRS away from the optic disc, and 3 (6.0%) eyes with MRS. The eyes with PVRS

around the optic disc had longer AL ($P < 0.001$), lower SE ($P < 0.001$), larger PPA area ($P < 0.001$), and thinner macular ChT ($P < 0.001$) than the eyes without retinoschisis (Supplementary Table S1). Multivariate regression analysis revealed that the presence of PVRS around the optic disc was negatively associated with macular ChT after adjustments for age, sex, AL, and PPA area (β , 95% confidence interval [CI], $\beta = -21.15$, 95% CI = $-37.69, -4.62$, $P = 0.012$, and adjusted R^2 of 0.185). We further found that longer AL (OR = 1.97, 95% CI = 1.42, 2.73, $P < 0.001$), the presence of

incomplete PVD (OR = 2.15, 95% CI = 1.01, 4.60, $P = 0.048$), and the presence of MAM (OR = 5.46, 95% CI = 1.99, 15.02, $P = 0.001$) were risk factors for PVRS around the optic disc.

Discussion

To the best of our knowledge, this is the first study to describe the distribution of PVAs among young adults with HM and to investigate their relationship with both macular ChT and vitreoretinal abnormalities. A decreasing trend of macular ChT was found in the eyes with PMs only, the eyes with both PCs and PMs, and the eyes with PLHs, PCs, and PMs. Additionally, the susceptibility of PVRS around the optic disc was evaluated. Longer AL, the presence of incomplete PVD, and the presence of MAM were risk factors for the occurrence of both PCs and PMs and for that of PVRS around the optic disc. This is a significant clinical observation given that the continuous thinning of macular ChT may lead to myopic maculopathy. PVAs and PVRS were commonly found in young HM eyes and were associated with both macular ChT and vitreoretinal abnormalities. These findings suggest that the presence of PVAs and PVRS could serve as a potential indicator for myopia progression at an early stage.

In our study, we identified PMs, PCs, and PLHs in 31.5%, 21.9%, and 4.7% of the HM eyes, respectively. In previous hospital-based investigations with approximate mean ages of 50 years, incidence of PMs was 44.6% to 82.9%, of PCs 48.4% to 71.7%, and of PLHs 14.0% to 31.4%.^{3,6,8} The values of our data were lower than those of most of the previous studies, in part because we focused on young adults, and other factors, such as OCT instrument, scanning mode and range, age group, definition of high myopia, and eye surgery history might have affected the detection accuracy of PVAs.²⁸ We further investigated the proportions of PVAs in different age groups and the proportions of the eyes with PMs, PCs, and PLHs were all found to increase with aging.

Our results revealed that in all eyes with PCs, the condition was accompanied by PMs and in all eyes with PCs and PMs, the disorders were accompanied by PLHs. We speculated there is a certain progressive relationship in the development of these three lesions. Choroid thinning is an important indicator for the progression of high myopia and pathologic myopia.^{14,16,17} Thus, we grouped the three lesions and found a decreasing trend of macular ChT in the eyes with PMs only, the eyes with both PCs and PMs, and the eyes with PLHs, PCs, and PMs. No significant

differences were found in macular ChT between the eyes with PMs only and the eyes without PVAs, whereas the eyes with PCs and PLHs and the eyes with PLHs, PCs, and PMs were found to be significantly associated with thinner macular ChT. Moreover, the concurrent presence of PLHs, PCs, and PMs was associated with a more significant decrease in macular ChT ($\beta = -34.12$, $P = 0.001$) than with the presence of both PCs and PMs ($\beta = -18.30$, $P = 0.001$). Thus, considerable attention should be paid to the presence of PCs or PLHs, but not of PMs only because they were closely associated with choroid thinning and probably with future myopia progression, which requires a further longitudinal study to confirm.

The development processes of PVAs and retinoschisis have been widely discussed, but the findings are still inconclusive.^{3,9} In general, PMs are the most common types of PVAs that occur with aging due to the insufficient flexibility of the retinal vessels and the action of tractional forces caused by the vitreous body.^{4,22} As lesions progress, PCs appear around PMs, and PLHs develop as the inner wall of PCs is removed by vitreoretinal forces. Our statistical analysis results revealed that incomplete PVD was no longer a risk factor for PLHs, which was consistent with the results of a previous study, suggesting that the formation of PLHs may be caused by the tractional force release from the retinal surface.⁷ Therefore, we propose that PLHs and PVRS are both advanced lesions of PCs. PLHs result from the release of the tractional force, whereas continuous vitreoretinal adhesions may induce PVRS (Fig. 3).^{7,9} The formation of PLHs and the defect of the inner retina in the eyes with PLHs could induce the migration of paravascular cells.^{3,9} The migrated cells might then

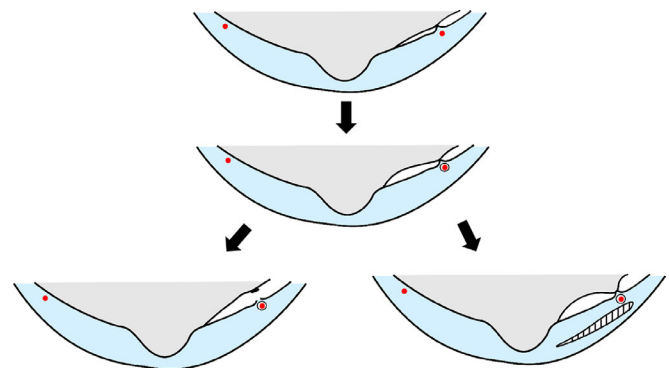


Figure 3. Schematic diagram showing the possible course of development of paravascular abnormalities and retinoschisis. First, paravascular microfolds (PMs) occur with aging, frequently accompanied by the vitreoretinal adhesion at the retinal vessel. Second, paravascular cystoid spaces (PCs) appear around PMs. Third, paravascular lamellar holes develop as the inner wall of PCs is removed by the vitreoretinal force, or paravascular retinoschisis occurs with continuous vitreoretinal adhesion.

produce collagen and facilitate the proliferative and contractive properties of the inner limiting membrane, which may play an important role in the development of MRS.³

Another interesting finding is that the largest part of the cases with retinoschisis in young HM eyes was with PVRs located around the optic disc. Few studies have examined peripapillary retinoschisis in HM eyes; thus, our research provided additional evidence in this field.^{29–31} Decreased macular and peripapillary ChT and increased PPA area have been reported in HM eyes.^{32–34} In the present study, we found that macular ChT was associated with further thinning, and the PPA area was additionally enlarged after the occurrence of peripapillary retinoschisis. According to previous studies, the enlargement of the PPA area and some morphological characteristics of the optic disc could precede the changes of the macula and were potential indicators of the progression of high myopia to pathologic myopia.^{35–38} Our results revealed that the presence of PVRs around the optic disc was independently associated with macular ChT, suggesting that it is an early indicator for myopia progression. Recently, Takahashi et al.⁷ proposed that retinoschisis may first appear in the paravascular area and then extend toward the macula. In the present study, in all three eyes with MRS, the condition coexisted with PVRs, and continuous trend for transition from PVRs to MRS was observed. Therefore, PVRs should also be considered a precursor lesion of MRS.

Several limitations in this study should be acknowledged. First, a referral bias might have existed because the recruitment was not population-based, and the results of this study could not be directly applied to young adults with HM in the general population. Second, due to the cross-sectional nature of this study, the progression of PVAs over time could not be investigated. To determine the causal effects for these lesions, a further longitudinal study is necessary. Third, the occurrence of posterior staphyloma was not assessed in our study due to its low prevalence in young people and the relatively insufficient SS-OCT scan length, accompanied by the absence of a wide-field imaging system.

In conclusion, PVAs can be observed in approximately one third of young adults with HM. The largest part of retinoschisis in young HM eyes is PVRs located around the optic disc. Longer AL, the presence of incomplete PVD, and the presence of MAM are potential risk factors for PVAs and PVRs around the optic disc. Our findings emphasize the importance of paying more attention to young HM eyes with PCs, PLHs, or PVRs, which are independently associated with choroidal thinning and might be potential indicators for myopia progression.

Acknowledgments

Supported by the National Key R&D Program of China (Project Nos. 2016YFC0904800, 2019YFC0840607, and 2019YFC1710204), the Shanghai Municipal Commission of Health (Public Health System Three-Year Plan Subjects; Project Nos. GWV-10.1-XK7 and GWV-10.2-YQ40), the National Natural Science Foundation of China (Project Nos. 81703287 and 81970846), the Clinical Science and Technology Innovation Project of Shanghai Shenkang Hospital (Project Nos. SHDC12019X18 and SHDC12020127), the Research Project of Shanghai Health Committee (Project No. 2019240241), the National Science and Technology Major Project of China (Project No. 2017ZX09304010), and the Medicine Science/Engineering Hybrid Project of Shanghai Jiaotong University (Project No. YG2019ZDA26).

Disclosure: **M. Li**, None; **L. Ye**, None; **G. Hu**, None; **Q. Chen**, None; **D. Sun**, None; **H. Zou**, None; **J. He**, None; **J. Zhu**, None; **Y. Fan**, None; **X. Xu**, None

* ML and LY contributed equally as co-first authors.

† JZ and YF contributed equally as co-corresponding authors.

References

1. Liu HY, Hsieh YT, Yang CM. Paravascular abnormalities in eyes with idiopathic epiretinal membrane. *Graefes Arch Clin Exp Ophthalmol*. 2016;254(9):1723–1729.
2. Muraoka Y, Tsujikawa A, Hata M, et al. Paravascular inner retinal defect associated with high myopia or epiretinal membrane. *JAMA Ophthalmol*. 2015;133(4):413–420.
3. Shimada N, Ohno-Matsui K, Nishimuta A, et al. Detection of paravascular lamellar holes and other paravascular abnormalities by optical coherence tomography in eyes with high myopia. *Ophthalmology*. 2008;115(4):708–717.
4. Sayanagi K, Ikuno Y, Gomi F, Tano Y. Retinal vascular microfolds in highly myopic eyes. *Am J Ophthalmol*. 2005;139(4):658–663.
5. Ohno-Matsui K, Hayashi K, Tokoro T, Mochizuki M. Detection of paravascular retinal cysts before using OCT in a highly myopic patient. *Graefes Arch Clin Exp Ophthalmol*. 2006;244(5):642–644.

6. Li T, Wang X, Zhou Y, et al. Paravascular abnormalities observed by spectral domain optical coherence tomography are risk factors for retinoschisis in eyes with high myopia. *Acta Ophthalmol.* 2018;96(4):e515–e523.
7. Takahashi H, Tanaka N, Shinohara K, et al. Importance of Paravascular Vitreal Adhesions for Development of Myopic Macular Retinoschisis Detected by Ultra-Widefield OCT. *Ophthalmology.* 2021;128(2):256–265.
8. Kamal-Salah R, Morillo-Sanchez MJ, Rius-Diaz F, Garcia-Campos JM. Relationship between paravascular abnormalities and foveoschisis in highly myopic patients. *Eye (Lond).* 2015;29(2):280–285.
9. Takahashi H, Nakao N, Shinohara K, et al. Posterior vitreous detachment and paravascular retinoschisis in highly myopic young patients detected by ultra-widefield OCT. *Sci Rep.* 2021;11(1):17330.
10. Ohno-Matsui K, Kawasaki R, Jonas JB, et al. International photographic classification and grading system for myopic maculopathy. *Am J Ophthalmol.* 2015;159(5):877–883.e877.
11. Deng J, Li X, Jin J, et al. Distribution Pattern of Choroidal Thickness at the Posterior Pole in Chinese Children With Myopia. *Invest Ophthalmol Vis Sci.* 2018;59(3):1577–1586.
12. Read SA, Fuss JA, Vincent SJ, Collins MJ, Alonso-Caneiro D. Choroidal changes in human myopia: insights from optical coherence tomography imaging. *Clin Exp Optom.* 2019;102(3):270–285.
13. Ikuno Y. Overview of the complications of high myopia. *Retina.* 2017;37(12):2347–2351.
14. Ikuno Y, Tano Y. Retinal and choroidal biometry in highly myopic eyes with spectral-domain optical coherence tomography. *Invest Ophthalmol Vis Sci.* 2009;50(8):3876–3880.
15. Zhou LX, Shao L, Xu L, Wei WB, Wang YX, You QS. The relationship between scleral staphyloma and choroidal thinning in highly myopic eyes: The Beijing Eye Study. *Sci Rep.* 2017;7(1):9825.
16. Zhou Y, Song M, Zhou M, Liu Y, Wang F, Sun X. Choroidal and Retinal Thickness of Highly Myopic Eyes with Early Stage of Myopic Chorioretinopathy: Tessellation. *J Ophthalmol.* 2018;2018:2181602.
17. Jin P, Zou H, Zhu J, et al. Choroidal and Retinal Thickness in Children With Different Refractive Status Measured by Swept-Source Optical Coherence Tomography. *Am J Ophthalmol.* 2016;168:164–176.
18. Ye L, Chen Q, Hu G, et al. Distribution and association of visual impairment with myopic maculopathy across age groups among highly myopic eyes - based on the new classification system (ATN). *Acta Ophthalmol.* 2022;100:e957–e967.
19. Ruiz-Medrano J, Montero JA, Flores-Moreno I, Arias L, Garcia-Layana A, Ruiz-Moreno JM. Myopic maculopathy: Current status and proposal for a new classification and grading system (ATN). *Prog Retin Eye Res.* 2019;69:80–115.
20. Takahashi H, Tanaka N, Shinohara K, et al. Ultra-Widefield Optical Coherence Tomographic Imaging of Posterior Vitreous in Eyes With High Myopia. *Am J Ophthalmol.* 2019;206:102–112.
21. Itakura H, Kishi S. Evolution of vitreomacular detachment in healthy subjects. *JAMA Ophthalmol.* 2013;131(10):1348–1352.
22. Ikuno Y, Gomi F, Tano Y. Potent retinal arteriolar traction as a possible cause of myopic foveoschisis. *Am J Ophthalmol.* 2005;139(3):462–467.
23. Dai Y, Jonas JB, Huang H, Wang M, Sun X. Microstructure of parapapillary atrophy: beta zone and gamma zone. *Invest Ophthalmol Vis Sci.* 2013;54(3):2013–2018.
24. Vianna JR, Malik R, Danthurebandara VM, et al. Beta and Gamma Peripapillary Atrophy in Myopic Eyes With and Without Glaucoma. *Invest Ophthalmol Vis Sci.* 2016;57(7):3103–3111.
25. Tay E, Seah SK, Chan SP, et al. Optic disk ovality as an index of tilt and its relationship to myopia and perimetry. *Am J Ophthalmol.* 2005;139(2):247–252.
26. Shin HY, Park HY, Park CK. The effect of myopic optic disc tilt on measurement of spectral-domain optical coherence tomography parameters. *Br J Ophthalmol.* 2015;99(1):69–74.
27. Bennett AG, Rudnicka AR, Edgar DF. Improvements on Littmann's method of determining the size of retinal features by fundus photography. *Graefes Arch Clin Exp Ophthalmol.* 1994;32(6):361–367.
28. Sayanagi K, Morimoto Y, Ikuno Y, Tano Y. Spectral-domain optical coherence tomographic findings in myopic foveoschisis. *Retina.* 2010;30(4):623–628.
29. Shimada N, Ohno-Matsui K, Nishimuta A, Tokoro T, Mochizuki M. Peripapillary changes detected by optical coherence tomography in eyes with high myopia. *Ophthalmology.* 2007;114(11):2070–2076.
30. Chebil A, Ben Achour B, Maamouri R, Ben Abdallah M, El Matri L. Peripapillary changes detected by SD OCT in eyes in high myopia. *J Fr Ophthalmol.* 2014;37(8):635–639.

31. Nishijima R, Ogawa S, Nishijima E, Itoh Y, Yoshikawa K, Nakano T. Factors Determining the Morphology of Peripapillary Retinoschisis. *Clin Ophthalmol*. 2021;15:1293–1300.
32. Song A, Hou X, Zhuo J, Yu T. Peripapillary choroidal thickness in eyes with high myopia. *J Int Med Res*. 2020;48(4):300060520917273.
33. Gupta P, Cheung CY, Saw SM, et al. Peripapillary choroidal thickness in young Asians with high myopia. *Invest Ophthalmol Vis Sci*. 2015;56(3):1475–1481.
34. Chen Q, He J, Yin Y, et al. Impact of the Morphologic Characteristics of Optic Disc on Choroidal Thickness in Young Myopic Patients. *Invest Ophthalmol Vis Sci*. 2019;60(8):2958–2967.
35. Fang Y, Yokoi T, Nagaoka N, et al. Progression of Myopic Maculopathy during 18-Year Follow-up. *Ophthalmology*. 2018;125(6):863–877.
36. Kim TW, Kim M, Weinreb RN, Woo SJ, Park KH, Hwang JM. Optic disc change with incipient myopia of childhood. *Ophthalmology*. 2012;119(1):21–26.e21–.
37. Guo Y, Liu L, Tang P, et al. Progression of myopic maculopathy in chinese children with high myopia: A long-term follow-up study. *Retina*. 2021;41(7):1502–1511.
38. Samarawickrama C, Mitchell P, Tong L, et al. Myopia-related optic disc and retinal changes in adolescent children from Singapore. *Ophthalmology*. 2011;118(10):2050–2057.